AIAA JOURNAL
Vol. 30, No. 7, July 1992

Study of Separated Shear Layer in Moderate Reynolds Number Plane Sudden Expansion Flows

M. Volkan Otugen* and George Muckenthaler†
Polytechnic University, Farmingdale, New York 11735

The turbulent structure of the incompressible separated shear layer behind a backward-facing step was studied experimentally. The growth of the shear layer, the development of dominant frequencies in the velocity spectra, and the evolution of large-scale structures were analyzed at various Reynolds numbers and expansion ratios. The downstream channel height-to-upstream channel height ratio was varied between 1.5 and 3.13. Independent of the expansion ratio, the Reynolds number based on the inlet channel height was varied between 6000 and 16,600. The streamwise velocity and the cross-correlation functions were measured using hot-wire anemometry. Faster growth rates observed at larger expansion ratios seem to be caused by the increased strength and size of the coherent structures inside the separated shear layer. Multiple interactions of these organized structures (pairing processes) are limited only to higher Reynolds numbers and larger expansions. In general, higher Reynolds numbers and smaller expansion ratios lead to higher shear layer Strouhal frequencies.

Nomenclature

b = upstream channel height
E = spectral energy at f
f = frequency
h = step height
L = integral length scale
R = time-space correlation function
Re = Reynolds number based on b and U_0
St = Strouhal number
t = time
U = mean streamwise velocity
u = fluctuating streamwise velocity
u' = root mean square of u
W = step span
x = streamwise distance measured from step
y = transverse distance measured from top of step
z = spanwise distance measured from midpoint of step
Δt = time delay in correlation function
Δz = spanwise separation distance in correlation function
δ^* = boundary layer displacement thickness at step
δ_w = shear layer vorticity thickness
η = nondimensional coordinate $\eta = y/x$

Subscripts

0 = reference condition measured upstream of step
m = local maximum value

Introduction

FLOWS with separated-reattached regions are commonly encountered in engineering practice. An example is the flow over a backward-facing step in a channel which finds applications in combustors and turbomachinery passages. Apart from its engineering relevance, the flow over a backward-facing step has attracted the attention of researchers as a model to analyze the more general problem of turbulent separation and reattachment as well. While the geometry is perhaps the simplest possible and the separation point is fixed, the structure of this flow still exhibits most of the features of the more complex geometries.

Despite the considerable attention it has received, certain aspects of the turbulent flow downstream of a backward-facing step in a channel are not well understood. This is particularly true of the unsteady flow behavior (encountered even in the statistically stationary flow) and the role of the large, coherent structures that develop immediately downstream of separation and tend to persist beyond reattachment. Flow reattachment and redevelopment strongly depend on the behavior of the initial shear layer separated from the step edge.[1] The shear layer structure is quite complex and is significantly different from that of a turbulent plane mixing layer. Unlike the plane mixing layer, the separated shear layer over a backward-facing step is influenced not only by the strong adverse pressure gradient, but also by the streamline curvature and the presence of a highly turbulent recirculating flow beneath it.[2] The initial shear layer is quite unstable and it quickly develops large-scale, span-aligned, roll-up structures that, by some accounts, start to interact at short distances from the step.[3-5] As a result, both the shear layer and its reattachment show low-frequency unsteadiness, even in statistically stationary flows, as observed by many researchers. For example, flow reattachment visualizations by Kim et al.,[6] separated shear-layer velocity measurements by Eaton and Johnston,[7] and Driver et al.,[5] all in turbulent flows downstream of a backward-facing step, indicated low-frequency, high-amplitude flow fluctuations. Driver et al.[5] conjectured that this low-frequency motion, observed in the region between separation and reattachment, was caused by the formation and subsequent multiple pairings of the large, coherent structures in the shear layer, while the study of Pronchick and Kline[3] indicated that the organized structures more or less disappear beyond three step-heights downstream from the step with no evidence of pairing beyond this distance.

Although it is clear that spanwise organized structures do exist in the turbulent separated shear layer, their exact nature and their influence on the separated shear-layer characteristics and reattachment is not well understood. This is partially due to the fact that various flow and geometry parameters significantly influence the flow over a backward-facing step. For example, the study by Isomoto and Honami[8] indicated that boundary layer and freestream turbulence upstream of the step has an effect on the flow development. Larger turbulence intensities result in shorter reattachment lengths. Adams and Eaton[9] found that larger boundary-layer thicknesses

Received May 23, 1991; revision received Oct. 23, 1991; accepted for publication Nov. 29, 1991.

*Assistant Professor, Aerospace Engineering Department. Member AIAA.
†Graduate Assistant, Aerospace Engineering Department.

at step edge result in lower reattachment pressure gradients and smaller shear-layer turbulence intensities. Recently, Otugen[10] investigated the effect of expansion ratio on the structure of the separated flow and subsequent reattachment past a backward-facing step. In this study, all flow parameters at the step were kept constant and the expansion ratio [ER = 1 + (*h*/*b*)] was varied between ER = 1.5 and 3.13 by changing the step height. The results indicated a dependence of the shear-layer characteristics on expansion ratio. Larger expansion ratios led to higher shear-layer turbulence intensities. It was concluded that the increase in turbulence activity led to the more rapid development of the shear-layer velocity profiles observed at larger expansion ratios, which in turn resulted in slightly shorter reattachment lengths. However, no mean flow mechanism could be identified to cause the observed alteration of turbulence development in the separated shear layer with varying expansion ratio. The time mean reattachment length variation from case to case was under 4.5% and, thus, was unlikely to create a significant change in the mean shear-layer streamline curvature. Furthermore, the evolution of the normalized streamwise pressure gradients remained invariant for different expansion ratios, excluding the adverse pressure gradient as the cause of the shear-layer turbulence intensity variation with expansion ratio.

The present experimental study was undertaken to further investigate the structure of the incompressible turbulent separated shear layer at multiple expansion ratios and to analyze the effect of this parameter, as well as the Reynolds number, on the formation and development of large-scale, organized structures. The measurements were performed in a moderate Reynolds number range varying between 6000 and 16,600. It is most likely that these organized structures control the turbulence and growth of the shear layer and, thus, are the key to understanding the expansion ratio effects. Extensive velocity measurements were made to analyze the power spectral distribution of the streamwise fluctuating velocity in the shear layer. Conditionally obtained space-time correlation functions were used to analyze the spanwise distribution of these structures. The Reynolds number and the expansion ratio were varied independently. For a fixed Reynolds number, all flow parameters at the step were kept constant. These include freestream velocity and turbulence intensity and, boundary-layer type (turbulent in all cases) and thickness. This was achieved by using a fixed inlet channel configuration, while varying the downstream channel height.

Experimental Facility and Technique

The wind tunnel in the study of Otugen[10] was used in the present experiments. The schematic of the tunnel is shown in Fig. 1. The open-circuit, low-speed tunnel has Plexiglas windows and operates in the suction mode. The blower, which is situated at the exit of the wind tunnel is coupled with the tunnel via vibration-inhibiting material to prevent the introduction of facility-driven instabilities in the flow. The air, drawn from the laboratory environment, enters the settling chamber through a set of honeycombs and fine mesh screens. The settling chamber, contraction nozzle, and straight wall leading to the step are all constructed as one piece to avoid surface discontinuities. However, enough surface roughness exists at the nozzle section leading to the step side wall to ensure rapid development of turbulence in the boundary layer. The downsteam channel is connected to the first piece through a flange. Therefore, when the two pieces are connected, the step, which is a part of the upstream piece, resides in the downstream channel, as shown in Fig. 1. The larger channel is fitted by a platform that serves as the lower wall of this downstream channel. Variable expansion ratios are obtained by raising or lowering the platform. The largest expansion ratio (ER = 3.13) is obtained by removing the platform from the channel. The wind tunnel provides a two-dimensionsal flow at the step at various Reynolds numbers and expansion ratios. For each Reynolds number, the flow conditions are maintained constant at the step, while varying the expansion ratio. These include the boundary-layer thickness and the turbulence intensity in both the freestream and the boundary layer. (Details of the wind tunnel can be found in Ref. 10.)

Flow conditions for various geometries are summarized in Table I. As indicated in this table, both the freestream and the boundary-layer turbulence intensities remained nearly constant throughout the experiments. The state of the boundary layer at the step edge was carefully investigated before the separated shear-layer measurements. In addition to the fairly high turbulent intensities obtained inside the boundary layer, time series analysis of streamwise velocity, measured around the location $y/\delta^* = 0.5$, indicated a nonintermittent (intermittency factor of one) turbulent flow with well-developed power spectral distributions that lacked large spikes or humps.

Velocity records were obtained using multiple channels of constant temperature hot-wire anemometry (TSI 1050) equipped with linearizers. The miniature tungsten sensors were 5-μ in diameter (TSI model 2160). The frequency response of each system was adjusted to approximately 20 kHz, which was above the maximum sampling rate. Because the objective of the study was to analyze the structure of the separated shear layer, the hot-wire measurements were confined to this

Table 1 Summary of inlet flow parameters

ER	*Re*	U_0, m/s	δ^*, mm	Freestream u'/U_0	BL[a] u'/U_0
1.5	10,000	9.64	0.81	0.0078	0.0841
	16,600	16.00	0.73	0.0071	0.0889
	6,000	5.78	0.86	0.0083	0.0790
2.0	10,000	9.64	0.81	0.0078	0.0841
	11,400	11.00	0.78	0.0077	0.0829
	16,600	16.00	0.73	0.0071	0.0889
3.13	10,000	9.64	0.81	0.0078	0.0841
	16,600	16.00	0.73	0.0071	0.0889

[a]Measured at $y/\delta^* = 0.5$.

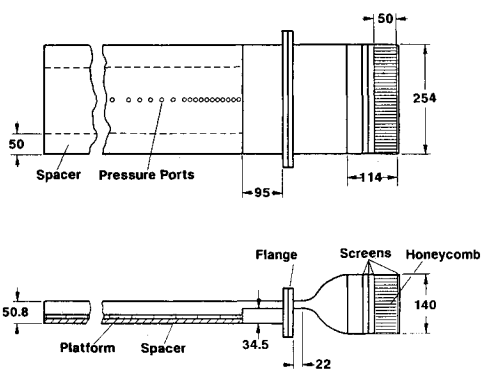

Fig. 1 Schematic of wind tunnel (all dimensions in mm).

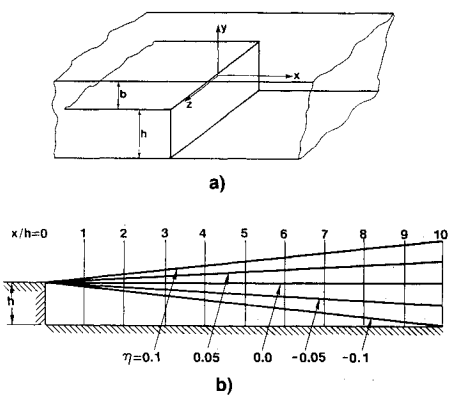

Fig. 2 Coordinate system for the step flow.

region and flow reversals in the recirculating region were avoided. The broader flowfield was mapped previously using a frequency shifted LDA and the possible zones of negative velocity were identified for a large set of parameters.[10] The wall static pressure was monitored through 0.8-mm static pressure taps on the step-side wall. The pressure taps were connected to a variable reluctance pressure transducer via a 24-port switching system (Scanivalve). The pressure readings were monitored throughout each experiment to ensure a constant flow rate (the unsteady flow fluctuations were approximately 1.5% of mean flow rate).

Central to the data acquisition system was an IBM 80286-based personal computer. The computer was equipped with a DAS-16F twelve bit, eight channel analog-to-digital converter with a maximum sample rate of 80,000/s. The statistically stationary properties of the flow, such as mean velocity and turbulence intensity, were analyzed on-line and displayed. For this, a typical rate of 200 samples per second was used with total record lengths of up to 30 s. A typical rate for the velocity spectra measurements was 5000 samples per second with one section of total duration.

The flow configuration is shown in Fig. 2. For the power spectral and cross-correlation distributions, hot-wire measurements were made at constant $\eta = x/y$ lines. This was done to allow for the growth of the shear layer when comparing flow characteristics at different streamwise locations.

The time-space correlation functions of the streamwise fluctuating velocity were obtained to analyze the spanwise distributions of the roll-up structures. These functions were evaluated through ensemble-averaging by selecting only the times in the velocity records when the passage of a large structure was detected. For this purpose, a single hot-wire sensor provided the trigger signal that was used in addition to the two sensors necessary for the correlation measurement. The sensor used as the trigger is fixed at a location ($y/h = 0$; $x/h = 0.5$, and $z/w = 0$) and provides instantaneous streamwise velocity information at this location. The two measurement sensors also provide instantaneous velocity information, but they can be traversed in the flow. The trigger signal and the two measurement signals are sampled simultaneously and stored for postprocessing. Record lengths of up to four minutes were typical. A positive velocity peak in the trigger signal, which was greater than twice the standard deviation of the record, was identified as the passage of a large structure. The selection of the threshold value for triggering is somewhat arbitrary and is obtained through trial measurements. The same criterion was successfully used by both Bruun[11] and Zaman and Hussain[12] in their study of the axisymmetric mixing layer. Only a small time window (usually less than 50 ms) around each large scale passage was included in the ensemble averaging to obtaining the correlation functions. In a record of four minutes, the trigger signal identified an average of 800 large structures.

Results and Discussion

The growth of the separated shear layer was determined from the mean streamwise velocity profiles. The profiles were measured for expansion ratios ranging between ER = 1.5 and 3.13 and at a fixed Reynolds number of 16,600. In all these measurements, the flow conditions at the step edge were kept constant (see Table I). The evolution of the constant U/U_m lines of the shear layer are shown in Fig. 3. For each case, both the streamwise and transverse distances are normalized by the step height. Near the step, the shear layer is thinner at larger expansion ratios. However, note that the absolute boundary-layer thickness at step is constant for each case, thus, resulting in a smaller relative shear-layer thickness around the initial separation region for larger step heights. The shear-layer growth rate is significantly increased at larger expansion ratios. By $x/h = 1.8$, the relative thickness of the shear layers are approximately equal and by $x/h = 3.6$, the

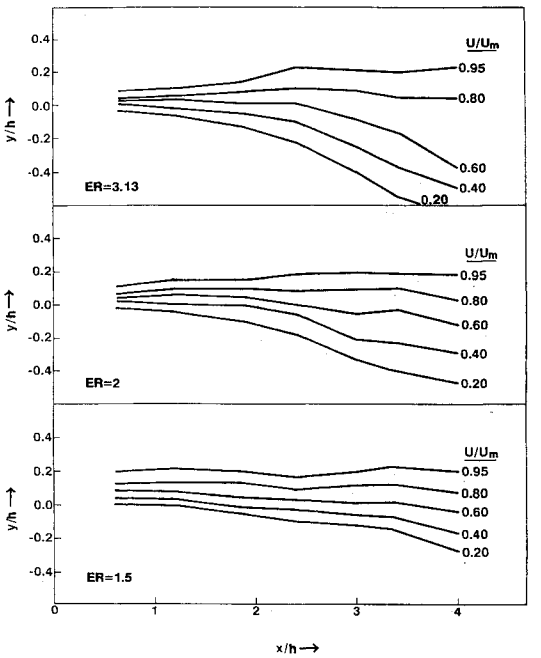

Fig. 3 Evolution of constant U/U_m lines.

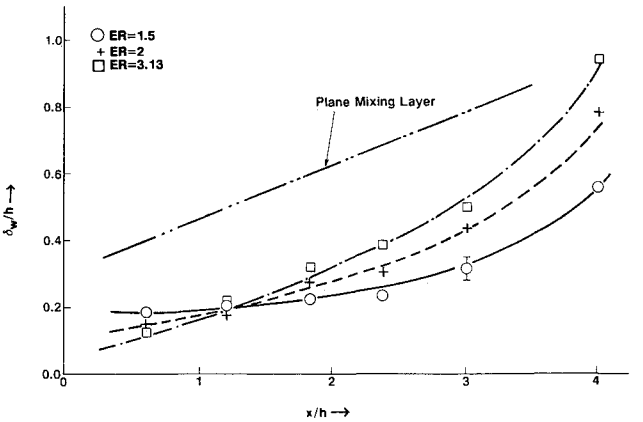

Fig. 4 Growth of the shear-layer vorticity thickness.

thickness of the shear layer for the largest expansion is more than twice that of the smallest expansion ratio. This is consistent with the earlier study of Otugen,[10] which showed that larger expansion ratios also led to significantly higher turbulence intensities, especially in the initial stages of separation. In that study, reattachment was determined as the location where long records of streamwise velocity obtained adjacent to the step side wall (using an LDA) showed 50% negative values. Although shorter normalized reattachment lengths were observed at larger expansions, the percent difference between the smallest and the largest expansion case was less than 4.5. Therefore, even if Fig. 3 were replotted with the streamwise distance normalized by the corresponding reattachment length, the growth patterns for the three expansion ratios shown would not collapse.

The vorticity thickness of the shear layer is shown in Fig. 4 for three expansion ratios. Again, the Reynolds number for all three cases is 16,600. The vorticity thickness is defined as:

$$\delta_w = U_0 / \left| \frac{\partial U}{\partial y} \right|_m$$

where

$$\left| \frac{\partial U}{\partial y} \right|_m$$

is the absolute value of the maximum mean shear obtained at each streamwise position. It is seen that cases with larger *ER* values exhibit faster growth rates of the normalized vorticity thickness. In Fig. 4, the vorticity thickness for the asymptotic region of a plane mixing layer (with an arbitrary virtual origin) is also shown to contrast the present shear-layer results. Unlike that of the simple mixing layer, the vorticity thickness of the shear layer separated from a backward-facing step in a channel grows in a nonlinear fashion. This strong nonlinearity in growth is due to the influence of certain global mechanisms that exist in the present flow, which are absent in the simple mixing layer. These mechanisms include; a reversed flow zone beneath the shear layer, giving rise to an intrinsically larger average normalized velocity difference between the two sides of the shear layer; curving of the streamlines; and the strong adverse pressure gradient.

The longitudinal integral length scales in the separated shear layer are calculated from velocity records obtained at $\eta = 0$. First, the integral time scales were calculated from the autocorrelation functions. These were then transformed into the length scales using Taylor's hypothesis. The convective velocity used for the transformation was the mean streamwise velocity at the respective location. Although the data in Fig. 5 show some scatter, it is evident that the integral length scale grows approximately linearly with streamwise distance. Furthermore, larger expansion ratios lead to slightly larger integral length scales consistent with the shear-layer growth-rate trends. However, the linear growth rate of the integral scale is somewhat surprising in view of the strongly nonlinear growth rate of the shear layer (vorticity) thickness shown in Fig. 4. This points to a lack of a strong relationship between the mean shear and the integral length scale of turbulence in the shear layer.

Larger expansion ratios lead to higher turbulence intensities in the initial region of the separated shear layer.[10] This, in turn, results in a faster growth rate. However, up to this point, it is unclear why an increase in the expansion ratio leads to increased shear-layer turbulence intensity. To investigate this issue further, we looked next at the evolution of instability frequencies and large-scale structures inside the shear layer. In this part of the study, power spectral distributions of the velocity as well as the time-space correlation functions were studied at various Reynolds numbers and expansion ratios. Samples of power spectra were obtained on various η lines in the separated shear layer. Generally, for a fixed set of flow conditions and x/h, power spectra obtained at positive η locations showed stronger peaks at a given instability frequency. This is depicted in Fig. 6. Here, the power spectra obtained at $x/h = 1.5$ for the expansion ratio of ER = 2 and $Re = 6000$ are shown. The spectral signature of the large structures is stronger on the upper portion of the shear layer, near the low-turbulence freestream. This was observed in almost all cases, and was particularly significant closer to the step edge. In the lower portion of the shear layer, the high turbulence

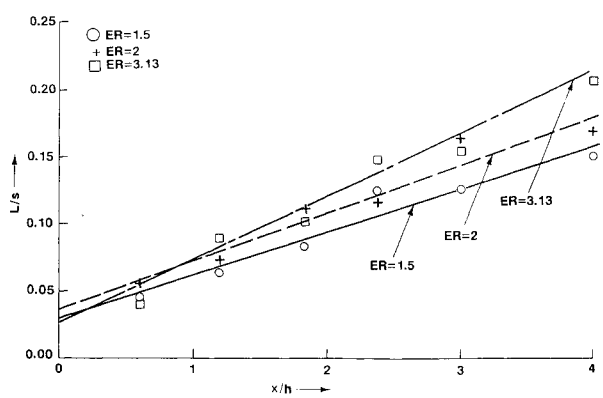

Fig. 5 Longitudinal integral scale distribution in shear layer.

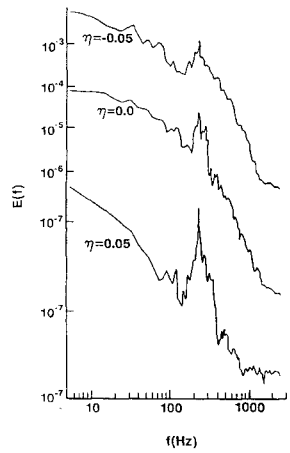

Fig. 6 Power spectral distribution of velocity at $x/h = 1.5$ (Re = 6,000 and ER = 2).

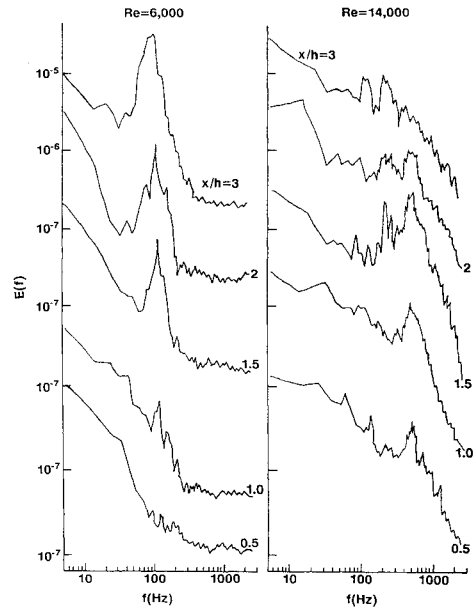

Fig. 7 Streamwise evolution of velocity spectra for ER = 2.

levels near the recirculation zone contribute to the spectra and tend to mask the dominant frequencies. To avoid the edge of shear layer and still have significant frequency peaks, a compromise location of $\eta = 0$ was chosen for the detailed spectra and Strouhal frequency analysis. Therefore, unless stated otherwise, all results presented below correspond to the nondimensional coordinate of $\eta = 0$.

At a fixed expansion ratio of ER = 2, velocity spectra were analyzed at multiple Reynolds numbers. Figure 7 is a sample showing the evolution of spectra with streamwise distance for the Reynolds numbers of 6000 and 14,000. These distributions represent the various features of the separated shear layer observed also at other flow conditions. In general, with increasing Reynolds numbers, the dominant frequency peaks become weaker and broader, as observed also by Berbee and Ellzey[13] in a similar flow configuration. This may indicate a less orderly behavior of the coherent structures at larger Reynolds numbers as a consequence of higher rates of jitter in the production and convection of large scales. However, for all Reynolds number cases, distinct frequency bands existed and a peak frequency could be determined. The higher the Reynolds number, the sooner (closer to the step) the shear-layer instabilities develop. In Fig. 7, a dominant mode forms (at 500 Hz) as early as $x/h = 0.5$ for $Re = 14{,}000$, while for $Re = 6000$, only a small peak (at 106 Hz) is observed at $x/h = 1$. It also seems that the evolution of the velocity spectra

is faster at higher Reynolds numbers. It is seen that for the low Reynolds number, the fundamental frequency is still developing at $x/h = 3$. On the other hand, for $Re = 14{,}000$, a subharmonic at 221 Hz is evident along with the fundamental frequency of 445 Hz as early as 1.5 step heights downstream, indicating a pairing process of the large-scale structures. Moreover, at $x/h = 3$, the fundamental frequency is completely replaced with the two subharmonics (210 Hz and 107 Hz), strongly suggesting the completion of the original pairing and the initiation of a second pairing. The multiple pairings observed in this study and their dependence upon the Reynolds number and expansion ratio are discussed further in the presentation of the Strouhal frequencies.

Next, the dependence of velocity spectra on the expansion ratio is studied. It was observed that higher expansion ratios lead to stronger peaks in the spectra. This indicates a more violent breakdown of the shear layer and the formation of stronger and better organized structures at larger expansion ratios. For example, the spectral distributions (at $x/h = 1$ and $Re = 16{,}600$) obtained at three ER values are compared in Fig. 8. It is clear that stronger peaks of the principal frequency occur at larger ER values. This may be the cause of the higher initial separated shear-layer turbulence intensities previously obtained at larger expansions. If one assumes that the energy content of the incoherent component of turbulence is fixed for different expansions (which Fig. 8 seems to indicate), stronger vortex structures will have higher stream velocity fluctuations at their passage, which will lead to increased turbulence intensities. Of course, stronger organized structures will also promote large-scale momentum mixing and shear-layer spread, as indicated in Fig. 3.

The velocity spectra obtained for a large set of Reynolds numbers and three expansion ratios were analyzed for dominant frequencies. From these, the corresponding Strouhal numbers are calculated. The Strouhal number is defined as: $St = fh/U_0$ where, f is a dominant frequency. The results are summarized in Fig. 9. In general, the Strouhal number decreases with increasing streamwise distance. This is consistant with the fact that, at larger streamwise distances, the passage frequency of the large structures decreases as the shear layer expands, and the convective velocity is reduced. Furthermore, for a fixed expansion (ER = 2), higher Reynolds numbers lead to larger Strouhal numbers. The same trend was observed by Berbee and Ellzey[13] in a study with ER = 1.33 and a similar range of Reynolds numbers. When the Reynolds number was fixed at 16,600, this time larger expansion ratios lead to somewhat smaller Strouhal numbers. Perhaps a more important feature indicated in Fig. 9 is the halving of the Strouhal frequency (or emergence of the subharmonic frequencies) only at certain cases. The Strouhal frequency halving is an

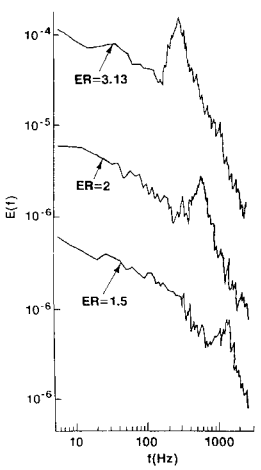

Fig. 8 Behavior of velocity spectra at $x/h = 1$ for three expansion ratios ($Re = 16{,}600$).

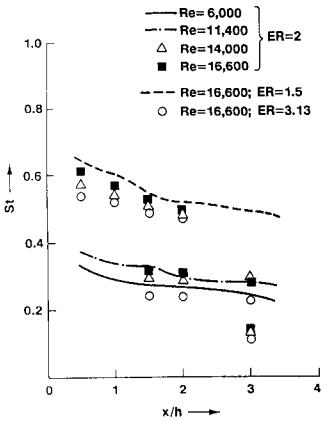

Fig. 9 Strouhal number evolution in the separated shear layer.

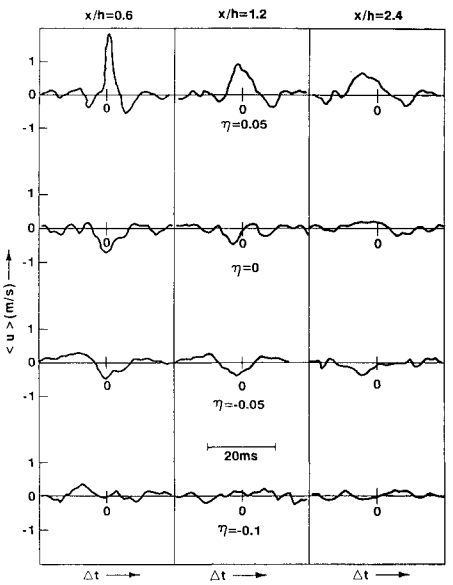

Fig. 10 Ensemble-averaged fluctuating velocity for ER = 2 and $Re = 16{,}600$.

indication of the pairing (or merging) of adjacent large-scale structures.[14] Such processes are known to be responsible for enhanced global mixing and shear-layer growth in turbulent flows. The process of vortex pairing in separated flows past a plane backward-facing step has been previously observed by some researchers,[3,5] while the data of others show no pairing process.[13] These experiments have been carried out under a diverse set of flow conditions and there is no clear evidence to indicate which conditions lead to the promotion or inhibition of such large-scale structure interaction.

In Fig. 9, the flow conditions that exhibited pairing processes are represented with symbols; whereas, for cases that showed no pairing, curved lines are used. For ER = 2, the two larger Reynolds numbers show a pairing process at both $x/h = 1.5$ and 3; whereas, for the two smaller Reynolds numbers, no pairing process is evident. On the other hand, for the fixed $Re = 16{,}600$, only the two larger expansion ratios are associated with a multiple pairing process. These results are interesting because, as mentioned earlier, it is known that the pairing of large coherent structures in turbulent flows leads to enhanced turbulent activity and shear-layer growth, as observed in mixing layers.[14] Therefore, this may explain the increasing turbulence intensities and shear-layer growth rates experienced at larger expansions.

The ensemble-averaged, streamwise fluctuating velocity $\langle u \rangle$ is shown in Fig. 10. These averages are obtained at various locations in the shear layer, and each column in the figure represents a single streamwise position. At each streamwise

position, four different η lines are chosen. The ensemble averaging is achieved by including in the average instantaneous values of u, occurring only when the trigger signal indicates the existence of a large-scale structure. In this way, an average history of u is obtained at the time-window when a large structure develops. The trigger sensor location is $x/h = 0.5$; $y/h = 0$; $z/W = 0$. Time $t = 0$ corresponds to the occurrence of a trigger signal. At $\eta = 0.05$ line, a fairly strong positive $\langle u \rangle$ persists even at a large distance of $x/h = 2.4$, indicating an orderly convection of the large-scale structures. Although the values weaken fairly quickly across constant η lines, a negative correlation value is clearly seen at $\eta = 0$. This is significant because it describes the positioning of the large-scale structures in the initial shear layer close to the step ($x/h < 1.2$). It seems that, positioned at $\eta = 0$, the measurement sensor is observing the lower portion of the roll-up structure, which creates a velocity deficit at its passage. Therefore, the structure is centered above the step-line $y = 0$, and the shear layer has not moved significantly toward the lower wall in this early stage. At $\eta = -0.1$, $\langle u \rangle$ is virtually zero, indicating a noncoherent fluctuating flow in this lower portion of the shear layer and, thus, the lack of influence of the organized structures above.

Next, the space-time correlation of velocity is obtained using two hot-wire probes separated from one another by varying distances along the spanwise coordinate Δz. A trigger sensor is used also to signal the passage of a large structure, again placed at the same location as before. The space-time correlation function is described as $R[\Delta z, \Delta t] = \langle u[x, y, z, t]\, u[x, y, (z + \Delta z), (t + \Delta t)] \rangle$ where Δt and Δz are the time-delay and separation distance, respectively. Again, an ensemble-averaging is used to obtain R, which takes into account only times when a structure is detected by the trigger probe. The variation of the correlation function with spanwise separation distance is shown in Fig. 11 for a streamwise position of $x/h = 0.6$. (Note that all the correlation measurements were made around the midplane of the wind tunnel.) All the peaks are centered around $t = 0$, indicating no phase delay as the separation distance is increased. This shows that, at least in the midsection of the tunnel where the measurements were made, the large structures are not inclined (or curved) in the spanwise direction. From Fig. 11, it can also be deduced that the spanwise extent of the average roll-up structure is larger than $0.8h$. Such correlation functions were obtained at various streamwise locations and for different expansion ratios, but are too extensive to be presented in this report. In summary, these results are similar to that in Fig. 11 and significant spanwise correlations persist at least up to $x/h = 4$ for various Re and ER cases. These results, therefore, are consistent with the earlier findings of Ruderich and Fernholtz[15] and Jovic and Browne[16] who reported the persistence of span aligned structures even close to the location of flow reattachment in similar separated shear flows.

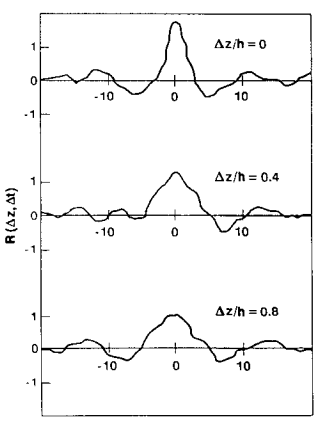

Fig. 11 Space-time correlation function for ER = 2 (Re = 16,600).

Conclusions

The primary objective of the present experimental work was the investigation of the turbulent separated shear-layer structure in a plane sudden expansion flow. The focus was on the effects of expansion ratio and the Reynolds number on this structure in the moderate Reynolds number range. Various expansion ratios were obtained with a fixed inlet configuration. Thus, at each Reynolds number, a fixed set of flow conditions were maintained at the step, while varying the expansion ratio. For each case, a turbulent boundary layer formed at the step. Both conditional and unconditional measurements of velocity were made using hot-wire anemometry.

In the range of Reynolds numbers and expansion ratios covered, measurements indicated the presence of large span-aligned structures inside the turbulent shear layer. From the spectral distributions of velocity, it was determined that the formation and evolution of the large-scale structures were accelerated with increasing Reynolds numbers. The same trend was observed with increasing expansion ratios, which also lead to more dominant frequency peaks in the power spectra. This is most likely an indication of increased strength of structures at larger expansions. Furthermore, multiple pairings of the large-scale structures is evident only at larger expansion ratios and Reynolds numbers. For the smallest expansion ratio and for $Re < 10{,}000$, no interaction of the large structures was evident. At larger Reynolds numbers and expansion ratios, the relatively thin shear layer develops instabilities sooner and breaks down into roll-up structures closer to the step. Subsequently, two adjacent structures coalesce (pairing process), which results in the halving of the structure passage frequency. Once the first pairing is completed, a second pairing process is initiated almost immediately after the first one, and this multiple-pairing process is completed within a streamwise distance of approximately four step-heights from the separation point. The results also indicate that larger Reynolds numbers and smaller expansion ratios lead to higher shear-layer Strouhal frequences.

It is known from the previous studies of the moderate Reynolds number plane mixing layers that the formation and interaction of span-aligned, large turbulent structures are linked with enhanced global momentum-mixing and shear-layer growth. The present results indicate the existence of a similar link also in the separated shear layer past a backward-facing step. It is believed that the faster growth rates observed at larger expansion ratios area caused by the intensified large-scale activity in the shear layer.

References

[1]Bradshaw, P., and Wong, F. Y. F., "The Reattachment and Relaxation of a Turbulent Boundary Layer," *Journal of Fluid Mech.*, Vol. 53, Part 1, 1972, pp. 113–135.

[2]Simpson, R. L., "Two-Dimensional Turbulent Separated Flow," North Atlantic Treaty Organization AGARD Rept. AG-287-Vol. 1, June 1985.

[3]Pronchick, S., and Kline, S., "An Experimental Investigation of the Structure of Reattaching Flow Behind a Backward-Facing Step," Stanford University, Mechanical Engineering Dept., Rept. MD-42, 1983.

[4]Roos, F. W., and Kegelman, J. T., "Control of Coherent Structures in Reattaching Laminar and Turbulent Shear Layers," *AIAA Journal*, Vol. 24, No. 12, 1986, pp. 1956–1963.

[5]Driver, D. M., Seegmiller, H. L., and Marvin, J. G., "Time-Dependent Behavior of a Reattaching Shear Layer," *AIAA Journal*, Vol. 25, No. 7, 1987, pp. 914–919.

[6]Kim, J., Kline, S. J., and Johnston, J. P., "Investigation of a Reattaching Turbulent Shear Layer: Flow Over a Backward-Facing Step," *Journal of Fluids Engineering*, Vol. 102, No. 2, 1980, pp. 302–308.

[7]Eaton, J., and Johnston, J., "Low Frequency Unsteadiness of a Reattaching Turbulent Shear Layer," *Proceedings of the Third International Symposium on Turbulent Shear Flows*, Davis, CA, Sept. 1981.

[8]Isomoto, K., and Honami, S., "The Effect of Inlet Turbulence Intensity on the Reattachment Process Over a Backward-Facing Step," *Journal of Fluids Engineering*, Vol. 111, No. 1, 1989, pp. 87–92.

[9]Adams, E. W., and Eaton, J. K., "An LDA Study of the Backward-Facing Step Flow Including the Effects of Velocity Bias," *Journal of Fluids Engineering*, Vol. 110, No. 2, 1988, pp. 275–282.

[10]Otugen, M. V., "Expansion Ratio Effects on the Separated Shear Layer and Reattachment Downstream of a Backward-Facing Step," *Experimental Fluids*, Vol. 10, No. 5, 1991, pp. 273–280.

[11]Bruun, H. H., "A Time-Domain Analysis of the Large Flow Structure in a Circular Jet. Part 1: Moderate Reynolds Number," *Journal of Fluid Mechanics*, Vol. 83, Part 4, 1977, pp. 641–671.

[12]Zaman, K. B. M. Q., and Hussain, A. K. M. F., "Natural Large Scale Structures in the Axisymmetric Mixing Layer," *Journal of Fluid Mechanics*, Vol. 138, 1984, pp. 325–346.

[13]Berbee, J. G., and Ellzey, J. L., "The Effect of Aspect Ratio on the Flow Over a Rearward-Facing Step," *Experiments in Fluids*, Vol. 7, No. 7, 1989, pp. 447–452.

[14]Winant, C. D., and Browand, F. K., "Vortex Pairing: The Mechanism of Turbulent Mixing Layer Growth at Moderate Reynolds Numbers," *Journal of Fluid Mechanics*, Vol. 63, Part 2, 1974, pp. 237–255.

[15]Ruderich, R., and Fernholz, H. H., "An Experimental Investigation of a Turbulent Shear Flow With Separation, Reverse Flow, and Reattachment," *Journal of Fluid Mechanics*, Vol. 163, 1986, pp. 283–322.

[16]Jovic, S., and Browne, L. W. B., "Coherent Structures in a Boundary Layer and Shear Layer of a Turbulent Backward-Facing Step Flow," Seventh Symposium on Turbulent Shear Flows, Stanford Univ., Aug. 21–23, 1989.